Publisher version DOI: 10.1109/JPHOTOV.2020.2998900



# Illumination-Dependent Requirements for Heterojunctions and Selective Contacts on Silicon

Brianna Conrad, Luca Antognini, Amalraj Peter Amalathas, Mathieu Boccard, and Jakub Holovský

***Abstract*—High efficiency silicon solar cells generally feature heterojunction or selective contact architectures, for which there is current interest in developing structures using a wide range of materials. The requirements that these layers must fulfill have been investigated previously for standard test conditions. Here we investigate how those requirements change under different illumination conditions. Heterojunction cells are fabricated and the effect of modified contact layers at different illumination levels is experimentally demonstrated. Simulations of a-Si/c-Si heterojunctions, and metal-semiconductor junctions reveal the dependence of the required electrode and contact layer work functions, and contact layer thickness, on the illumination level between 0.1 and 10 suns. The difference in requirements for cells which are intended for use in low light conditions, as tandem device sub-cells, or under low-level concentration is found.**

***Index Terms*—Carrier selective contacts, Heterojunctions, Photovoltaic cells, Silicon devices, Simulation**

## I. Introduction

As the quest for increasing efficiencies of silicon solar cells continues, attention has turned from traditional diffused homojunction cells to heterojunction (HJ) devices, such as the c-Si/a-Si HJ interdigitated back contact (IBC) cell that holds the current 26.7% AM1.5G conversion efficiency record [1], [2]. The TOPCon structure, which refers to a tunnel-oxide passivated selective contact made from poly-silicon (in other words, a poly-Si/c-Si heterojunction cell) has also achieved over 25% efficiency in a both-sides contacted device [3].

Despite these results, optical losses in the top layers of these devices are still significant, and have motivated the search for other materials which can be used to form selective contacts. The requirements for selective contacts from a variety of materials have been investigated using simulations by several groups [4]–[10]. Devices have been demonstrated with electron and hole contacts fabricated from metal oxides including MoOx [9]–[17], WOx [12]–[15], V2Ox [9], [12]–[15], [18], [19], NiOx, TiO2 [20], and ZnO [17], [21], as well as III-V semiconductors [22]–[24] and organic materials [20], [25]–[27], with varying levels of success at demonstrating high efficiencies.

B. Conrad, A. Peter Amalthas, and J. Holovský are with the Centre for Advanced Photovoltaics, Faculty of Electrical Engineering, Czech Technical University, 16627 Prague, Czech Republic.

L. Antognini and M. Boccard are with the Photovoltaics and Thin Film Electronics Laboratory , Institute of Microengineering, EPFL, CH-2000 Neuchâtel, Switzerland

B. Conrad email: bsmc@alum.mit.edu

J. Holovsky is also with the Institute of Physics, ASCR, 16200 Prague, Czech Republic.

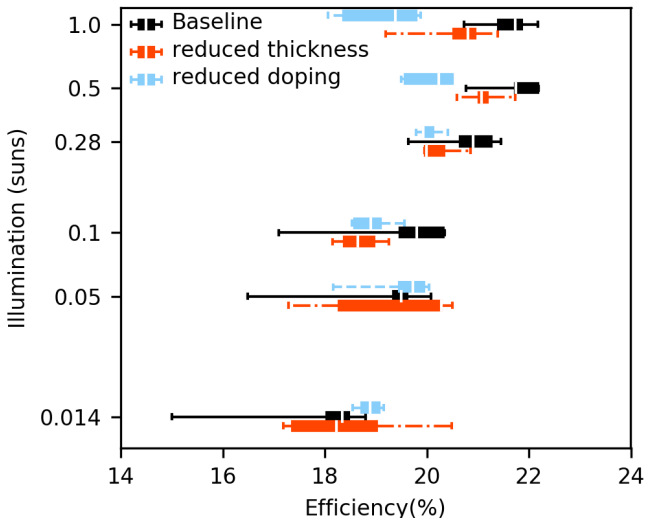


Fig. 1. Experimental efficiency at varying illumination levels for SiHJs fabricated according to a standard recipe, and with reduced a-Si doping and thickness. All devices were measured at the same nominal illumination levels; bars are offset slightly for readability.

Like most silicon solar cell research, these requirements and results are reported for 1-sun illumination conditions. There are, however, numerous situations in which deployed solar cells will be working at other illumination levels, including at high latitudes, under cloudy skies and during the morning or afternoon. In a tandem device with a III-V, perovskite or thin film top cell, operating under 1 sun, a silicon bottom sub-cell will experience reduced illumination. On the other hand, if low-level concentration is used for such a device, it may experience higher illumination.

Given that a primary concern for selective contacts is efficient carrier extraction [9] the amount of current which needs to be extracted (a function of illumination level) will affect the requirements for these contacts. It has been noted that devices are more sensitive to non-ideal contacts at higher illumination levels, and the Voc measured at 100 suns has been used as a stand-in for device performance at the more demanding maximum power point under 1-sun. 100x in this case has been chosen due to the availability of characterization equipment rather than for any fundamental reason [28]. There is as of yet, no quantitative exploration of how the illumination level affects the requirements of the materials used to form carrier selective contacts to silicon solar cells.

This work therefore investigates how the material requirements for a good selective contact for a silicon solar cell vary with illumination level. We can discover thereby to what extent

they might be relaxed in a tandem cell, or one designed for indoor use, or what extra requirements might be if the cell is to be used under concentration. SiHJ solar cells fabricated with varying emitter doping and thickness (alternatively, selective contact work function and thickness) and characterized at varying illumination levels, experimentally demonstrating this variation. Such measurements at illumination levels below 1 sun are rarely reported on.

Simulations are then used to quantitatively investigate how the material requirements for a good selective contact for a silicon solar cell vary with illumination level. We can discover thereby to what extent they might be relaxed in a tandem cell, or one designed for indoor use, or what extra requirements might be if the cell is to be used under concentration. We use simulations of a SiHJ solar cell and simplified structures that highlight the roles of different layers and interfaces to answer these questions. As mentioned, a SiHJ cell is essentially a selective contactact solar cell, and many conclusions from these simulations, especially those of simplified structures, are applicable to selective contacts made from other materials.

## II. Experimental Results

The resilience of devices to reduced doping (WF) and thickness at different illumination levels was demonstrated experimentally by the fabrication of SiHJ solar cells. 4 $cm^2$ P-on-N devices were fabricated according to a baseline recipe, with PECVD deposition time of the p-doped a-Si reduced to 2/3 of the baseline, and with the TMB dopant gas flow rate reduced to 1/5 of the baseline. The a-Si thickness for the reduced doping cells was measured to be the same as that of the reduced thickness cells, meaning that they have both reduced doping and thickness. Devices were then measured at different illumination levels from 0.014 suns to 1 sun using a 1-sun intensity solar simulator and hand-held neutral density filters. Maximum power points and efficiencies were extracted from I-V curves.

The spread of device efficiencies are plotted in Fig. 1. It is seen that reducing the contact layer thickness and WF (by way of doping) reduces device efficiency by a significantly greater amount at the higher illumination levels. At the lowest illumination levels it is not clear that it does so at all. The highest efficiencies are achieved at illumination levels below 1 sun. While series resistance losses may be a factor, IV curves also start to show the characteristic s-shape that indicates that current extraction is being limited by non-ideal contact properties (Fig. 2) [29]. In the following sections, the dependence on illumination levels of requirements for SiHJ solar cells and other selective contact devices are quantified through simulation studies.

## III. Simulation Methods

Selective contacts are investigated primarily through the lens of the p-type emitter of a SiHJ solar cell, which can alternatively be viewed as the hole-selective contact of this device. The conclusions are equally applicable to an electron-selective contact, with the appropriate adjustments, for example, a preference for low contact work functions (WFs) instead

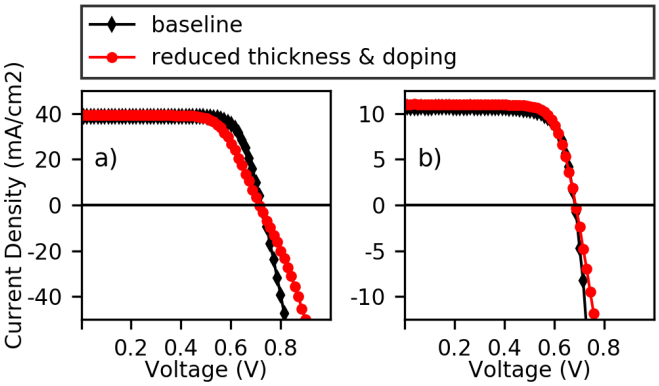


Fig. 2. Experimental IV curves for a representative baseline cell and cell with reduced contact doping and thickness at a) 1 sun and b) 0.28 suns.

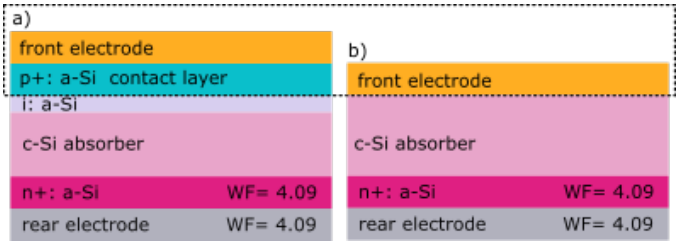


Fig. 3. The SiHJ structures simulated in AFORS-HET, with the layers whose properties are varied and investigated outlined. a) full device structure and b) MS junction variation used in Section III-A to investigate the basic WF requirement for a selective contact.

of high, and concern about barriers in the conduction band rather than in the valance band.

Simulations are carried out using AFORS-HET [30] software, with structures as shown in Fig. 3. The crystalline silicon absorber and the rear (electron) contact layers are unvaried throughout the study. The material properties of c-Si and a-Si are set from the materials provided in the software. This includes defects in the a-Si layers as described in Table 1. The WF of the front electrode and the thickness and WF (via doping level) of the p-type a-Si layer, which we will refer to as the contact layer, are varied throughout the work.

In these structures, the contact layer must have a suitable WF in its own right, and be able to screen any unsuitable properties of the metal or TCO electrode. The combination of contact and electrode properties must also be such that device performance is not limited by the interface between those two materials. To separate the requirements imposed by each of these aspects, simplified structures are simulated first. These include the metal-semiconductor (MS) junction shown in Fig. 3b and a SiHJ (Fig. 3a) with the electrode WF set equal to that of the contact layer. The details and results of these simulations, and how they reveal the effect of illumination levels on the requirements of SiHJ and selective contacts are presented in the following sections.

## IV. Simulations Results

### A. Simple Work Function Requirement

The simplest hole-selective contact is a single material with a high WF, such as the MS junction seen in Fig. 3b. This

TABLE I
DEFECTS IN SIMULATED A-SI LAYERS

| type | distribution | total concentration | electronic capture |
|---|---|---|---|
| Doped Layer | | | |
| donors | conduction tail, Urbach E = 0.12eV | 1.6e20 | $C_n$=$C_p$ = 7e-16 |
| acceptors | valance tail, Urbach E = 0.12eV | 2.4e20 | $C_n$=$C_p$ = 7e-16 |
| donors | Gaussian, center = 1.1eV, $\sigma$ = 0.21 | 6.9e19 | $C_n$= 3e-14, $C_p$=3e-15 |
| acceptors | Gaussian, center = 1.2ev, $\sigma$ = 0.21 | 6.9e19 | $C_n$=3e-15, $C_p$=3e-14 |
| Intrinsic Layer | | | |
| donors | conduction tail, Urbach E = 0.035eV | 6.4e19 | $C_n$=$C_p$ = 7e-16 |
| acceptors | valance tail, Urbach E = .05eV | 9.4e19 | $C_n$=$C_p$ = 7e-16 |
| donors | Gaussian, center = 0.89eV, $\sigma$ = 0.144 | 5.0e15 | $C_n$= 3e-14, $C_p$=3e-15 |
| acceptors | Gaussian, center = 1.09eV, $\sigma$ = 0.144 | 5.0e15 | $C_n$= 3e-14, $C_p$=3e-15 |

principle underlies the SiHJ and other selective contacts, and by studying this structure we can see the baseline requirements in any of these cases, without the influence of barriers to carrier extraction imposed by band discontinuities or tunneling currents limited by trap density. The structure is simulated with low surface recombination at the electrode/absorber interface and varying electrode WF.

The simulated open circuit voltage and efficiency of cells with different WFs are shown in Fig. 4a as a function of illumination level. An expected logarithmic relationship between the illumination level and the Voc is seen. As the electrode WF drops below 5.05eV, the Voc is decreased, and this is slightly more pronounced for higher illumination levels. We see a similar trend with the efficiency of the device, but with a more pronounced difference in the efficiency drop between low and high illumination levels. At 10 suns, an efficiency loss is already obvious with a 5.05eV electrode WF, whereas at 0.1 suns, a 5.00eV electrode WF shows no losses. As has been pointed out by previous authors [9], the maximum power point is more demanding than open circuit as the extraction of light generated current is required, and this demand increases as more current is extracted.

This relationship can be quantified by looking at the WF required to meet a certain benchmark at different illumination levels. Previous authors have used the difference between internal (Fermi level separation) and external voltage at the maximum power point ($\Delta V_{MP}$) to evaluate the quality of the contact, citing a relatively constant value of internal $V_{MP}$ [9], [31]. However, we found in this study that this consistency was dependent on the illumination level, with a larger portion of voltage losses occurring in the internal voltage as the illumination level decreases. Therefore, we consider the efficiency loss as compared to the bulk limited case, where further improving the contact properties resulted in no additional efficiency improvement. These losses are plotted in Fig. 5, wherein horizontal lines mark 0.36% loss. This value corresponds approximately to a 10mV drop, and was used as our condition for an acceptable contact. The electrode WFs where this condition is met (Fig. 6) show a logarithmic dependence on illumination levels, as

$$WF_{required} = WF_{1sun} + Aln(suns) \quad (1)$$

with values of $WF_{1sun}$ and A listed in Table II. From Fig. 5, one can see that changing the chosen requirement within a reasonable range shifting the horizontal lines up or down would preserve the logarithmic dependency, despite the different $WF_{1sun}$ value.

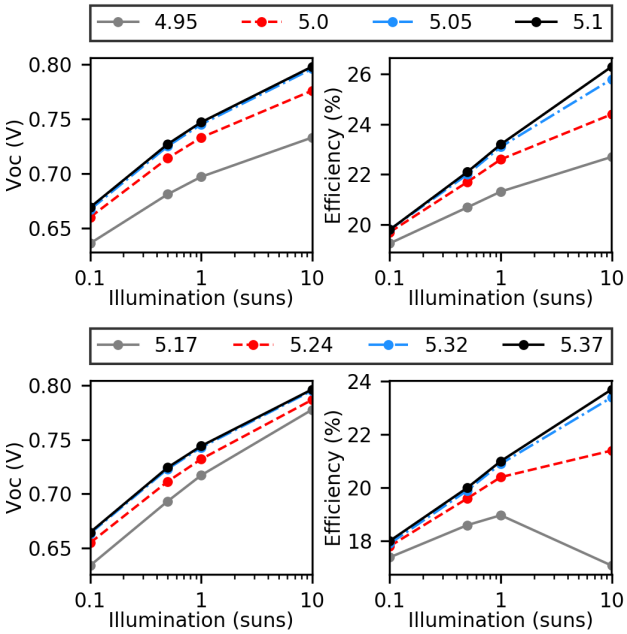


Fig. 4. a) Voc and Efficiency of solar cells based on metal-semiconductor junctions with a variety of electrode WFs between 0.1 and 10 suns. b) Voc and Efficiency of SiHJs with flatband electrode/contact interfaces and a range of contact layer WFs between 0.1 and 10 suns.

A real MS junction would, of course, be subject to additional constraints, namely high surface recombination and Fermi level pinning. If the surface recombination of this device is left high, the required WF increases and variation with illumination level is extremely small, as the device is dependent on the high WF for all passivation.

For the case with Fermi level pinning, the metal WF can be replaced by an effective work function (WF'): [32]

$$WF' = S(WF - E_{MG}) + E_{MG} \quad (2)$$

where $E_{MG}$ is the midgap energy of the c-Si absorber, and $S$ denotes the degree of pinning - 0 for full pinning and 1 for no pinning. Combining with Eqn. 1 the required electrode WF becomes

$$WF_{required} = \left[\frac{WF_{1sun}}{S} + E_{MG}(1 - \frac{1}{S})\right] + \frac{A}{S}ln(suns) \quad (3)$$

TABLE II
PARAMETERS FIT TO EQN. 1 FOR DIFFERENT STRUCTURES STUDIED

| Structure | $WF_{1sun}$ (eV) | A(meV) |
|---|---|---|
| MS junction | 5.02 | 218 |
| SiHJ | 5.27 | 310 |

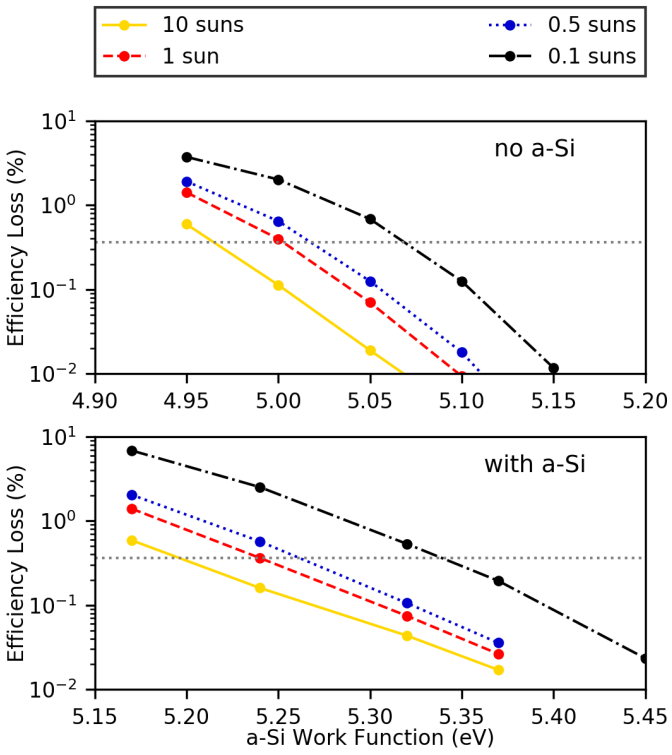


Fig. 5. Efficiency as a function of electrode WF in (a) a MS junction-based device and (b) a SiHJ with flatband interface between a-Si and electrode.

with the values of $WF_{1sun}$ and $A$ unchanged. As Fermi level pinning increases, so too do the required electrode WF at a given illumination, and the slope of the required WF with respect to illumination level. Full Fermi Level pinning results in Eqn. 3 being undefined, as changing the electrode WF has no effect on the effective WF, and therefore the required effective WF cannot be reached.

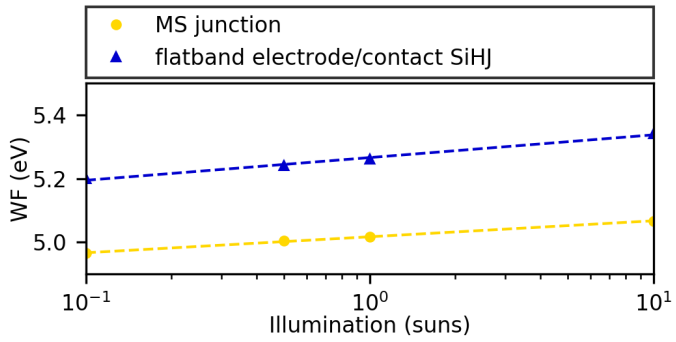


Fig. 6. Required WF to maintain an efficiency loss of 0.36% or less for a MS junction and a SiHJ with flatband a-Si/electrode interface. The first indicates the minimum WF required by any hole-selective contact.

### B. Overcoming Band Discontinuities

As compared to the MS junction considered above, the SiHJ solar cell (Fig. 3a) has the additional constraint that the band bending must be sufficient to overcome the barrier caused by the discontinuity in the valance band at the a-Si/c-Si interface. A failure to fulfill this condition leads to S-shaped I-V curves and dramatically reduced cell efficiencies, even when Voc may not be affected [29].

To investigate only the interaction between this a-Si layer and the c-Si absorber, we fixed the WF of the electrode to that of the a-Si layer, to create a flatband contact/electrode interface. The a-Si layer thickness was set to 13nm doped and 2nm intrinsic. The WF was varied by adjusting the a-Si doping level. The Voc and Efficiency results shown in Fig. 4b again show greater decrease due to low contact WF at high illumination levels, as well as higher WFs required to reach the limiting values than in the MS junction case.

With efficiency losses plotted as in the previous case (Fig. 5,6) a similar logarithmic relationship, as well as the need for higher WF contact layers, and a steeper dependence on illumination level compared to the MS junction, is seen. The parameters for Eqn. 1 fit to this data are also shown in Table II .

The results in these sections are also applicable to high WF n-type hole contacts which depend on tunneling to extract holes from the absorber valence band to the contact conduction band. These contacts have also been seen to result in s-shaped curves when current extraction is not sufficient [6], [11], [13], [16]. MoOx hole contacts have been shown to be well-modeled as metals when defect trap densities ($N_T$) are high enough to allow for sufficient trap-assisted tunneling, or when the WF is high enough to allow for band to band tunneling [7], [8], [33], making them equivalent to the MIS junction under that condition. Messmer *et al.* investigated the effect of varying both $N_T$ and WF in the trap-assisted regime, showing that at one sun, as log($N_T$) decreases, the WF-efficiency curve is shifted to higher WF values, but maintains the same shape [7]. From this we can surmise that for a given trap density the logarithmic dependence of the required WF on illumination will remain. As increasing log($N_T$) has the same effect on efficiency as increasing WF, a linear dependence on illumination level of required $N_T$ for a given WF can also be expected, though coefficients will vary. As the contact WF for which band to band tunneling becomes possible does not vary with illumination, and this process allows for high current extraction, the required WF will not increase beyond this point regardless of illumination level or trap density. Varying the passivation method and barriers to carrier extraction (e.g. by the inclusion of an i:a-Si layer) will effect the required WFs, whether operating in the trap-assisted or band-to-band tunneling region.

### C. Electrode/Contact Interface

Having investigated the interface between the contact layer and the absorber, we now look at the interface between the contact layer and the electrode. To do this we simulate a full SiHJ structure with an independent electrode WF such that

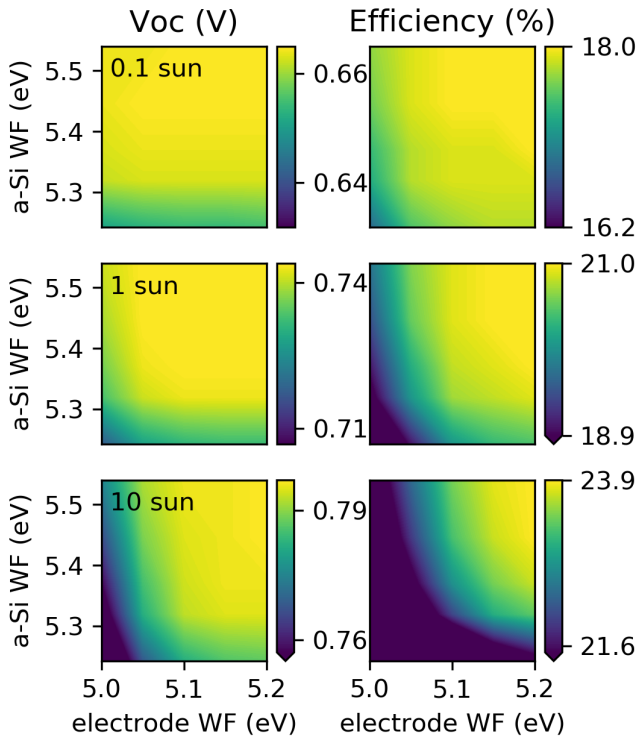


Fig. 7. Performance of realistic devices with thick contact layers and a range of electrode and contact layer WFs at different illumination levels. For each illumination level, the minimum values of the color range for Voc and Efficiency are set to 95 and 90% of the maximum, respectively, so illumination levels can be compared despite differing absolute scales.

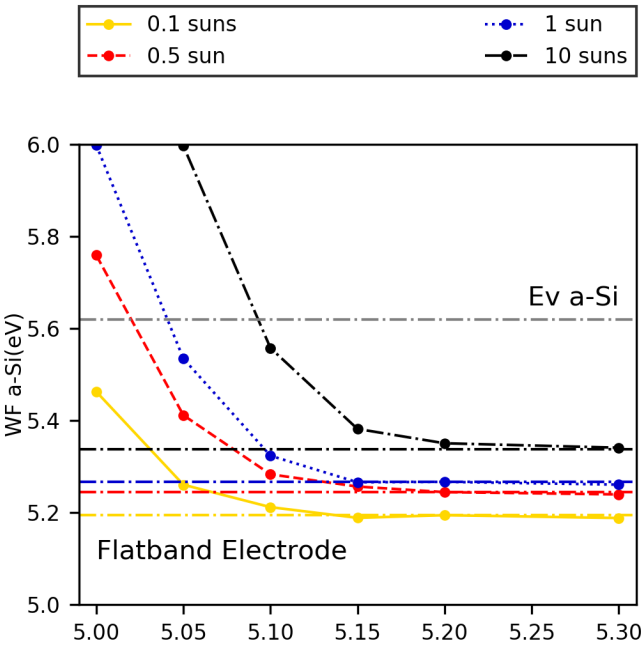


Fig. 8. Thickness of contact layer required to achieve 0.1% efficiency loss compared to a thick contact layer, with no absorption in the contact layer.

there is a WF difference between the electrode and the contact layer. We focus on the case where the contact layer WF is higher, resulting in a Schottky barrier at the interface.

Tunneling current through such a barrier increases as the barrier height and width decreases. This means that a smaller WF mismatch between contact layer and electrode (barrier height) and a higher doped contact layer (leading to a narrower barrier) both allow for increased current extraction.

Clearly, the best case is when both WFs are high. To investigate the behavior at different illumination levels when the WFs are reduced, simulations of full devices with thick a-Si layers (13nm doped/2nm intrinsic, as above) are performed. The thick contact layers ensure that the electrode will be fully screened. Fulfilling that condition will be addressed in the next section. Tunneling through the Schottky barrier is enabled in AFORS-HET.

Fig. 7 shows the effect on Voc and Efficiency of reducing either or both WFs at 0.1, 1, and 10 suns. At each illumination level, the minimum of the color bar is the same percent of the maximum, to allow for meaningful comparison. It is clear that reducing the electrode WF, and thereby increasing the Schottky barrier height, results in losses that are greater at higher illuminations. Increasing the contact layer WF improves the device, with a narrower barrier and better contact/absorber interface properties having a larger effect than the increased barrier height at the contact/electrode interface.

The minimum WFs necessary to fulfill the same 0.36% absolute efficiency loss condition introduced in the previous section are found and plotted in Fig. 8, with a comparison to the WF necessary with a flatband contact/electrode interface. Thereby, the cases where the contact/electrode interface is the limiting factor can be identified. This occurs when the electrode WF is below 5.15-5.3 eV, depending on the illumination level. For higher electrode WFs, the contact/absorber interface is the limiting factor, and there is no difference between this case and the flatband case. Inclusion of tunneling at the contact/absorber interface could raise the transition values, extending the range that is limited by the electrode/contact interface. As the electrode WF drops, a higher contact layer WF is required to maintain low losses, with a steeper increase at higher illumination levels. At 10 suns, as the electrode WF is reduced, the required contact WF quickly becomes higher than the valance band level of a-Si. This highlights the importance for application using even low concentration levels of recent explorations of higher WF electrode materials [34].

### *D. Contact Layer Thickness*

As previously mentioned, the contact layer must screen the electrode layer if the latter's WF is too low. This means that the contact layer must be thick enough to contain the band bending induced by the electrode layer, and return to a WF that is favorable for the contact/absorber interface. The distance over which this occurs in known as the Debye length:

$$L_D = \sqrt{\frac{k_B T}{q} \frac{\epsilon_s}{q N_Q}} \tag{4}$$

where $N_Q$ is the net fixed charge density in the semiconductor. Therefore the contact layer must have sufficient combination of thickness and charge density. It is important to note that this does not refer only to the ionized dopants, but to the total

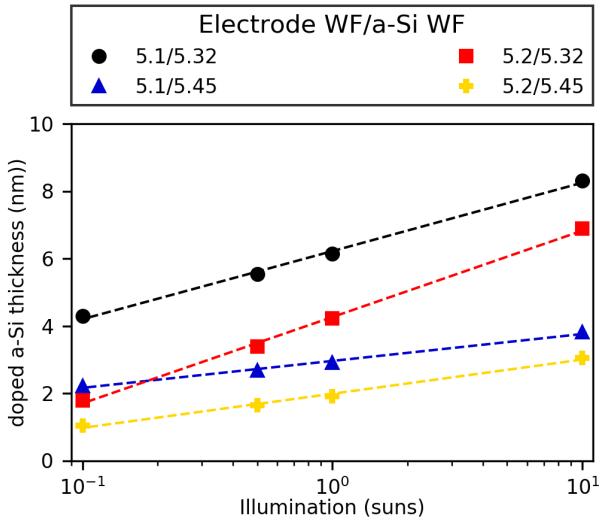


Fig. 9. Required WF to maintain an efficiency loss of 0.36% or less for a MS junction and a SiHJ with flatband a-Si/electrode interface. The first indicates the minimum WF required by any hole-selective contact.

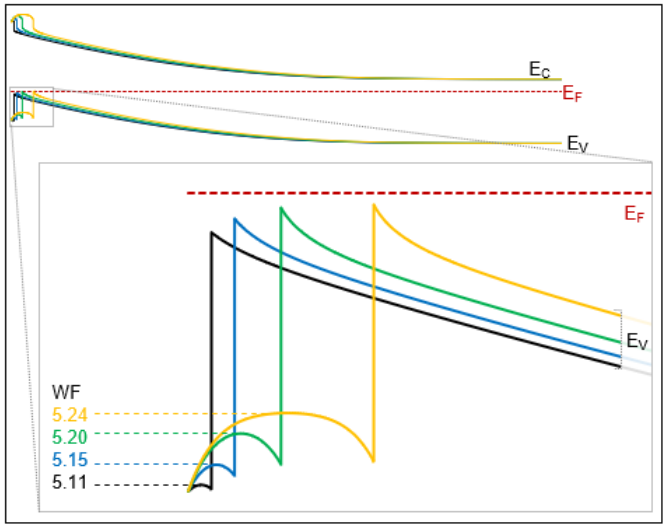


Fig. 10. Simulated band diagram with different contact layer thicknesses, showing partial screening and a reduced effective contact layer WF with thinner layers. This results in a thinner layer being needed at lower illumination levels.

space charge of this region as determined by the combination of ionized dopants and defects. Therefore, the screening lengths are considerably reduced by the presence of defects, as described by Varache *et al.* [5].

Devices were simulated with varying contact layer thicknesses for several WF combinations and illumination levels. Absorption in the contact layer was set to zero to allow for uncomplicated assessment of the electrical properties. The thicknesses required to reach 0.1% efficiency loss from that with a thick contact layer are plotted in Fig. 9. (Note that this considers screening length only, and not the effect of interfaces investigated previously. A fully screened electrode with a poor contact WF will still perform poorly). A logarithmic dependence of the required thickness on illumination level is seen. Thicker layers are required when the a-Si WF is lower (black circles and red squares). A steeper dependence of thickness on illumination level occurs when the electrode WF is higher, or the contact WF is lower.

The dependence on illumination level is interesting here, as there is nothing in the Debye length equation that depends on the illumination level. The charge density $N_Q$ is that of the fixed charges. The higher extraction rate at higher illumination levels does not significantly affect $N_Q$. Examination of the simulated band diagram with varying contact layer thicknesses (Fig. 10) shows the origin of the illumination dependence. In cases where the contact layer is thinner than the Debye length, the electrode WF will still be partially screened. There is a maximum WF reached before the band begins to bend back under the influence of the absorber, thereby creating an effective contact layer WF. As we showed previously, lower illumination levels require lower contact layer WFs. Therefore, a less complete screening of the electrode, and a thinner contact layer can be tolerated.

Fig. 11 shows the device efficiency with a 5.1eV electrode WF and two different contact layer WFs at different illumination levels for varying contact layer thicknesses. For

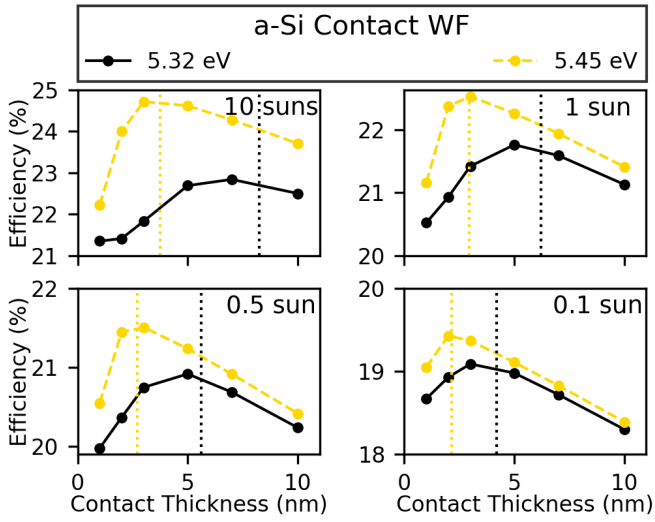


Fig. 11. Efficiency of devices with varying contact layer thickness. Minimum thicknesses needed for sufficient screening of electrodes are indicated with vertical dotted lines.

these simulations, absorption in the a-Si contact layer is once again included. The required screening thickness from the previous step is also indicated. The effect of reduced current from thicker layers is clearly seen, with ideal thicknesses that are slightly thinner than the screening thicknesses. The combination of a high WF and thin contact layer allows a closer approach to ideal than a lower WF and thicker layer. With absorption in the a-Si layer considered, illumination level affects the ideal thickness of the contact layer, with thicker layers stil preferred at higher illumination levels. The difference, however, becomes very small with high contact WF.

## V. Conclusion

Through AFORS-HET simulation of SiHJ solar cells and MS junctions we have quantitatively investigated selective contact requirements at different illumination levels. The contact layer WF and thickness requirement varies logarithmically with illumination for a given electrode WF. The slope of the trend is determined by factors that include band offsets and the chemical passivation of surfaces and interfaces. These results are applicable to contacts formed from other materials as well. In hole contacts which rely on band-to-band or trap-assisted tunneling, the band alignment which allows for highly efficient band-to-band tunneling will not vary with illumination. However, when trap-assisted tunneling is required, we expect similar logarithmic dependencies on illumination for the required contact WF and $\log(N_T)$. The details of this must be investigated in further work with simulation tools that allow for the inclusion of such processes. From this work it can be seen that higher WF materials are required for devices that operate under concentration, even at low levels, and that lower illumination applications can make use of devices containing a wider range materials, and thinner layers, as selective contacts.

Appendix one text goes here.

## Acknowledgment

This work was supported by the Czech Ministry of Education, Youth and Sports project CZ. 02.1.01/0.0/0.0/15_003/0000464 Centre of Advanced Photovoltaics.

## References

[1] K. Yoshikawa, H. Kawasaki, W. Yoshida, T. Irie, K. Konishi, K. Nakano, T. Uto, D. Adachi, M. Kanematsu, H. Uzu, and K. Yamamoto, "Silicon heterojunction solar cell with interdigitated back contacts for a photoconversion efficiency over 26%," *Nature Energy*, vol. 2, p. 17032, 2017.

[2] M. A. Green, E. D. Dunlop, D. H. Levi, J. Hohl-Ebinger, M. Yoshita, and A. W. Ho-Baillie, "Solar cell efficiency tables (version 54)," *Progress in Photovoltaics: Research and Applications*, vol. 27, no. 7, pp. 565–575, 2019.

[3] S. Glunz, F. Feldmann, A. Richter, M. Bivour, C. Reichel, H. Steinkemper, J. Benick, and M. Hermle, "The irresistible charm of a simple current flow pattern: 25% with a solar cell featuring a full-area back contact," in *31st EUPVSEC*, Hamburg, Germany, 2015.

[4] M. Bivour, B. Macco, J. Temmler, W. E. Kessels, and M. Hermle, "Atomic layer deposited molybdenum oxide for the hole-selective contact of silicon solar cells," *Energy Procedia*, vol. 92, pp. 443 – 449, 2016, proceedings of the 6th International Conference on Crystalline Silicon Photovoltaics (SiliconPV 2016).

[5] R. Varache, J. Kleider, M. Gueunier-Farret, and L. Korte, "Silicon heterojunction solar cells: Optimization of emitter and contact properties from analytical calculation and numerical simulation," *Materials Science and Engineering: B*, vol. 178, no. 9, pp. 593 – 598, 2013.

[6] R. A. Vijayan, S. Essig, S. De Wolf, B. G. Ramanathan, P. Löper, C. Ballif, and M. Varadharajaperumal, "Hole-collection mechanism in passivating metal-oxide contacts on si solar cells: Insights from numerical simulations," *IEEE Journal of Photovoltaics*, vol. 8, no. 2, pp. 473–482, March 2018.

[7] C. Messmer, M. Bivour, J. Schn, S. W. Glunz, and M. Hermle, "Numerical simulation of silicon heterojunction solar cells featuring metal oxides as carrier-selective contacts," *IEEE Journal of Photovoltaics*, vol. 8, no. 2, pp. 456–464, March 2018.

[8] H. Mehmood, H. Nasser, T. Tauqeer, S. Hussain, E. Ozkol, and R. Turan, "Simulation of an efficient silicon heterostructure solar cell concept featuring molybdenum oxide carrier-selective contact," *International Journal of Energy Research*, vol. 42, no. 4, pp. 1563–1579, 2018.

[9] M. Bivour, C. A. Messmer, L. Neusel, F. Zahringer, J. Schon, S. W. Glunz, , and M. Hermle, "Principles of carrier-selective contacts based on induced junctions," in *EUPVSEC 2017 Amsterdam*, 2017.

[10] H. Nasser, G. Kökbudak, H. Mehmood, and R. Turan, "Dependence of n-csi/moox heterojunction performance on csi doping concentration," *Energy Procedia*, vol. 124, pp. 418 – 424, 2017.

[11] C. Battaglia, S. M. de Nicolás, S. De Wolf, X. Yin, M. Zheng, C. Ballif, and A. Javey, "Silicon heterojunction solar cell with passivated hole selective moox contact," *Applied Physics Letters*, vol. 104, no. 11, p. 113902, 2014.

[12] M. Bivour, J. Temmler, F. Zähringer, S. Glunz, and M. Hermle, "High work function metal oxides for the hole contact of silicon solar cells," in *2016 IEEE 43rd Photovoltaic Specialists Conference (PVSC)*, June 2016, pp. 0215–0220.

[13] S. Essig, J. Dréon, J. Werner, P. Löper, S. De Wolf, M. Boccard, and C. Ballif, "Moox and wox based hole-selective contacts for wafer-based si solar cells," in *2017 IEEE 44th Photovoltaic Specialist Conference (PVSC)*, June 2017, pp. 55–58.

[14] L. G. Gerling, S. Mahato, A. Morales-Vilches, G. Masmitja, P. Ortega, C. Voz, R. Alcubilla, and J. Puigdollers, "Transition metal oxides as hole-selective contacts in silicon heterojunctions solar cells," *Solar Energy Materials and Solar Cells*, vol. 145, pp. 109 – 115, 2016.

[15] W. Wu, J. Bao, X. Jia, Z. Liu, L. Cai, B. Liu, J. Song, and H. Shen, "Dopant-free back contact silicon heterojunction solar cells employing transition metal oxide emitters," *physica status solidi (RRL) Rapid Research Letters*, vol. 10, no. 9, pp. 662–667, 2016.

[16] D. Sacchetto, Q. Jeangros, G. Christmann, L. Barraud, A. Descoeudres, J. Geissbühler, M. Despeisse, A. Hessler-Wyser, S. Nicolay, and C. Ballif, "Ito/moox/a-si:h(i) hole-selective contacts for silicon heterojunction solar cells: Degradation mechanisms and cell integration," *IEEE Journal of Photovoltaics*, vol. 7, no. 6, pp. 1584–1590, Nov 2017.

[17] F. Wang, S. Zhao, B. Liu, Y. Li, Q. Ren, R. Du, N. Wang, C. Wei, X. Chen, G. Wang, B. Yan, Y. Zhao, and X. Zhang, "Silicon solar cells with bifacial metal oxides carrier selective layers," *Nano Energy*, vol. 39, pp. 437 – 443, 2017.

[18] W. Wu, W. Lin, J. Bao, Z. Liu, B. Liu, K. Qiu, Y. Chen, and H. Shen, "Dopant-free multlilayer back contact silicon solar cells employing v2ox/metal/v2ox as an emitter," *RSC Advances*, vol. 7, pp. 23 851–23 858, 2017.

[19] G. Masmitja, L. G. Gerling, P. Ortega, J. Puigdollers, I. Martin, C. Voz, and R. Alcubilla, "V2ox-based hole-selective contacts for c-si interdigitated back-contacted solar cells," *Journal of Materials Chemistry A*, vol. 5, pp. 9182–9189, 2017.

[20] L. Yang, J. Chen, K. Ge, J. Guo, Q. Duan, F. Li, Y. Xu, and Y. Mai, "Polymer/si heterojunction hybrid solar cells with rubrene:dmso organic semiconductor film as an electron-selective contact," *The Journal of Physical Chemistry C*, vol. 122, no. 41, pp. 23 371–23 376, 2018.

[21] S. Zhong, M. Morales-Masis, M. Mews, L. Korte, Q. Jeangros, W. Wu, M. Boccard, and C. Ballif, "Exploring co-sputtering of zno:al and sio2 for efficient electron-selective contacts on silicon solar cells," *Solar Energy Materials and Solar Cells*, vol. 194, pp. 67 – 73, 2019.

[22] C. Zhang, E. Vadiee, R. R. King, and C. B. Honsberg, "Carrier-selective contact gap/si solar cells grown by molecular beam epitaxy," *Journal of Materials Research*, vol. 33, no. 4, pp. 414–423, 2018.

[23] M. Darnon, R. Varache, M. Descazeaux, T. Quinci, M. Martin, T. Baron, and D. Munoz, "Solar cells with gallium phosphide/silicon heterojunction," *AIP Conference Proceedings*, vol. 1679, no. 1, p. 040003, 2015.

[24] R. Blasco, A. Nunez-Cascajero, M. Jimenez-Rodriguez, D. Montero, L. Grenet, J. Olea, F. B. Naranjo, and S. Valdueza-Felip, "Influence of the alinn thickness on the photovoltaic characteristics of alinn on si solar cells deposited by rf sputtering," *physica status solidi (a)*, vol. 216, no. 1, p. 1800494, 2019.

[25] J. He, W. Zhang, J. Ye, and P. Gao, "16heterojunction solar cells using narrow band-gap conjugated polyelectrolytes based low resistance electron-selective contacts," *Nano Energy*, vol. 43, pp. 117 – 123, 2018.

[26] J. He, Y. Wan, P. Gao, J. Tang, and J. Ye, "Over 16.7% efficiency organic-silicon heterojunction solar cells with solution-processed dopant-free contacts for both polarities," *Advanced Functional Materials*, vol. 28, no. 34, p. 1802192, 2018.

[27] C. Reichel, U. Würfel, K. Winkler, H.-F. Schleiermacher, M. Kohlstädt, M. Unmüssig, C. A. Messmer, M. Hermle, and S. W. Glunz, "Electron-selective contacts via ultra-thin organic interface dipoles for silicon organic heterojunction solar cells," *Journal of Applied Physics*, vol. 123, no. 2, p. 024505, 2018.

[28] M. Bivour, M. Reusch, S. Schröer, F. Feldmann, J. Temmler, H. Steinkemper, and M. Hermle, "Doped layer optimization for silicon

heterojunctions by injection-level-dependent open-circuit voltage measurements," *IEEE Journal of Photovoltaics*, vol. 4, no. 2, pp. 566–574, March 2014.

[29] R. V. K. Chavali, J. R. Wilcox, B. Ray, J. L. Gray, and M. A. Alam, "Correlated nonideal effects of dark and light iv characteristics in a-si/c-si heterojunction solar cells," *IEEE Journal of Photovoltaics*, vol. 4, no. 3, pp. 763–771, May 2014.

[30] R. Varache, C. Leendertz, M. Gueunier-Farret, J. Haschke, D. Munoz, and L. Korte, "Investigation of selective junctions using a newly developed tunnel current model for solar cell applications," *Solar Energy Materials and Solar Cells*, vol. 141, pp. 14 – 23, 2015.

[31] M. Bivour, M. Reusch, F. Feldmann, M. Hermle, and S.Glunz, "Requirements for carrier selective silicon heterojunctions," in *24th Workshop on Crystalline Silicon Solar Cells & Modules: Materials and Processes*, Breckenridge, Colorado, 2014.

[32] W. Mnch, "Electronic properties of ideal and interfacemodified metalsemiconductor interfaces," *Journal of Vacuum Science & Technology B: Microelectronics and Nanometer Structures Processing, Measurement, and Phenomena*, vol. 14, no. 4, pp. 2985–2993, 1996.

[33] S. Chuang, C. Battaglia, A. Azcatl, S. McDonnell, J. S. Kang, X. Yin, M. Tosun, R. Kapadia, H. Fang, R. M. Wallace, and A. Javey, "Mos2 p-type transistors and diodes enabled by high work function moox contacts," *Nano Letters*, vol. 14, no. 3, pp. 1337–1342, 2014.

[34] F. Feldmann, K.-U. Ritzau, M. Bivour, A. Moldovan, S. Modi, J. Temmler, M. Hermle, and S. W. Glunz, "High and low work function materials for passivated contacts," *Energy Procedia*, vol. 77, pp. 263 – 270, 2015.